Field-induced nucleation in phase change memory

V. G. Karpov* and Y. A. Kryukov
Department of Physics and Astronomy, University of Toledo, Toledo, Ohio 43606, USA

I. V. Karpov and M. Mitra
Intel Corporation, RN3-01, 2200 Mission College Boulevard, Santa Clara, California 95052, USA
(Received 19 March 2008; revised manuscript received 31 July 2008; published 26 August 2008)

A theory of field-induced crystal nucleation is developed and verified experimentally for the case of switching in nanoglasses of phase change memory. For symmetry-breaking strong electric fields, it predicts needle-shaped crystallites with nucleation barriers lower than that of spherical nuclei and a strong field dependent. We have observed bias dependent switching for times and temperatures far beyond those typically reported and supportive of our predictions, in particular, switching time exponential in voltage and temperature.

DOI: 10.1103/PhysRevB.78.052201 PACS number(s): 61.43.Fs, 61.46.−w, 68.18.Jk, 73.63.−b

The recent developments in chalcogenide phase change memory (PCM) (Ref. 1) revived interest in the physics of crystal nucleation in glasses. We recall that PCM utilize electrically initiated reversible amorphous-to-crystalline phase changes in multicomponent chalcogenides such as $Ge_2Sb_2Te_5$ (GST); the markedly different phase resistances are used as the two logic states. Switching from the high- to low-resistive (crystalline) state is triggered by voltages exceeding a certain threshold value V_{th}. Physically, switching creates a cylinderlike crystalline inclusion shunting through the amorphous host.[2]

In his seminal work, Ovshinsky[3] suggested that switching "can be analyzed in terms of nucleation theory wherein the nucleation rate is dependent on the applied voltage." His hypothesis was then overshadowed by alternative explanations referring to electronic instabilities.[4] Here we revisit the nucleation switching concept and show that field-induced nucleation can evolve through the barriers substantially lower than the standard nucleation. We present experimental data verifying our predictions.

The field effect on nucleation is due to a conductive ("metal") nucleus whose strong polarization decreases the electrostatic energy W_E. These effects are more pronounced for nuclei elongated in the direction of the applied electric field,[5] which can be thought of as conducting prolate spheroids. The extremum cases of low and high fields will then correspond to spherical and needle-shaped nuclei, respectively. Their fields and electrostatic energies are described by the equation,[6]

$$E = E_0/n, \quad W_E = -\Omega E_0^2 \varepsilon/(8\pi n), \tag{1}$$

where ε is the dielectric permittivity of the host insulating phase, Ω is the conducting particle volume, and E_0 is the uniform field far from the particle. The depolarizing factor $n=1/3$ for a spherical particle, while for a prolate spheroid of length h and radius R ("needle") it becomes[6]

$$n = \frac{1-e^2}{2e^3}\left(\ln\frac{1+e}{1-e} - 2e\right), \quad e \equiv \sqrt{1-\left(\frac{2R}{h}\right)^2}. \tag{2}$$

The corresponding volume, surface area, and free energy are given by

$$\Omega = \frac{2\pi R^2 h}{3}, \quad A = 2\pi\left\{R^2 + \frac{Rh\arccos(2R/h)}{\sin[\arccos(2R/h)]}\right\}, \tag{3}$$

$$F_{sph} = A\sigma - \Omega\mu + W_E. \tag{4}$$

Here the first two terms represent the interface and bulk contributions with σ and μ being the surface tension and the chemical-potential difference between the two phases, respectively.

According to our theory, switching starts with nucleation of a needle-shaped crystal embryo. Similar to a lightning rod, it concentrates the electric field, which facilitates nucleation of additional particles at its end, etc. This instability leads to a low-resistive crystalline filament across the structure. The embryo induction time $\tau=\tau_0\exp(W/kT)$ is interpreted as the switching delay time.

As a baseline, consider first a spherical particle in the electric field E_0. Its free energy $F(R)=4\pi R^2\sigma-4\pi R^3\mu/3 - R^3E_0^2\varepsilon/2$ is a maximum at the nucleation barrier

$$W = W_0(1+\zeta/4)^{-2}, \quad \zeta \equiv E_0^2R_0^3\varepsilon/W_0, \tag{5}$$

where

$$R_0 = 2\sigma/\mu \quad \text{and} \quad W_0 \equiv 16\pi\sigma^3/3\mu^2 \tag{6}$$

are the zero-field critical nucleation radius and barrier, respectively. For numerical estimates, we use the typical[7] $W_0 \approx 2$ eV, $R_0 \approx 3$ nm, and $\varepsilon=16$ and the switching field strength $E_0 \approx 3\times10^5$ V/cm, which yields $\zeta \approx 0.1$; hence $W \approx W_0$, i.e., relatively small field effect.

Closed-form results can be as well obtained in the limiting case of needle-shaped spheroids $h/R \gg 1$, where

$$n = (R/h)^2[\ln(2h/R) - 1] \equiv (R/h)^2\Lambda, \tag{7}$$

$\Omega=2\pi R^2h/3$, $A=\pi^2Rh/2$, and the free energy becomes

$$F_N = \pi^2Rh\sigma/2 - 2\pi R^2h\mu/3 - h^3E_0^2\varepsilon/12\Lambda. \tag{8}$$

Because the parameter space here is two dimensional (R and h), the system can find nucleation pathways through lower barriers than the energy maximum as shown in Fig. 1.

According to both Fig. 1 [representing the exact free energy of Eq. (4)] and asymptotic Eq. (8), nucleation pathways

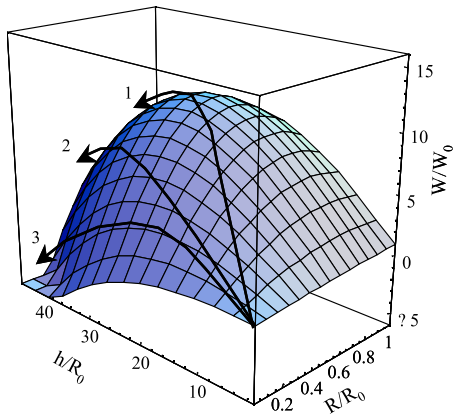

FIG. 1. (Color online) Free energy of a prolate spheroid nucleus [Eq. (4) with definitions from Eqs. (1)–(3)] as a function of the spheroid radius R and length h. The arrows illustrate possible nucleation pathways: 1 passes through the maximum nucleation barrier, 2 follows the transformation path with fixed ratio h/R, and 3 traverses yet lower nucleation barriers.

of small R's correspondingly traverse low barriers vanishing with $R \to 0$. In reality, several factors set lower bounds to the needle radius R. Such are, for example, the failure of the interfacial energy (σ) concept and mechanical stresses between the two phases capable of rupturing too thin needles. These size limitations will be phenomenologically accounted for by introducing a minimum radius (αR_0), below which the conductive crystalline cylinder does not exist; $\alpha(\ll 1)$ remains a dimensionless phenomenological parameter.

In the spirit of classical nucleation theory, an embryo evolution is described by a multitude of trajectories $R(h)$ in the parameter space (R,h) illustrated in Fig. 2. The free energy $F_N[R(h)]$ along each trajectory is given by Eq. (8) when $R \geq \alpha R_0$ and is a maximum at a particular "saddle" point determining the trajectory barrier. These barriers vary between different trajectories and we seek the minimum of them satisfying the condition $R \geq \alpha R_0$. As seen from Fig. 2, such a minimum belongs on the trajectory to which the line $R = \alpha R_0$ is a tangent. A unique nature of the above-defined

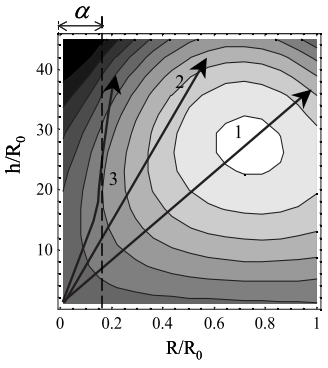

FIG. 2. Contour plot of the energy surface and nucleation trajectories from Fig. 1. Along each trajectory, the nucleus stability region is beyond its corresponding energy maximum (saddle) point. The minimum of that maximum energy point corresponds to trajectory 3, to which the dashed line $R/R_0 = \alpha$ is a tangent. Their touching at $R = R_0$ and $h = h_0$ determines the nucleation barrier.

nucleation barrier is that it is related to a saddle point formed by the intersection of the free-energy surface and the "wall" $R = \alpha R_0$, since the former surface itself does not have saddle points.

The touching point coordinates $R = \alpha R_0$, $h = h_0$, and energy W are determined by the equations $\min[R(h,W)] = \alpha R_0$ and $F_N(R,h) = W$. The latter can be represented in the form

$$\frac{3\pi}{8}\frac{R}{R_0} - \left(\frac{R}{R_0}\right)^2 = \frac{WR_0}{W_0 h} + \frac{h^2\zeta}{12R_0^2\Lambda}, \tag{9}$$

where we have taken into account the definitions from Eq. (6). Differentiating it with respect to h and setting $dR/dh = 0$ gives $h_0 = R_0(6W\Lambda/\zeta W_0)^{1/3}$ at $R = \alpha R_0$, where we have neglected the logarithmically weak dependence $\Lambda(h)$ treating Λ as a constant. Finally, substituting $h = h_0$ and $R = \alpha R_0$ into Eq. (9) and neglecting the term quadratic in $\alpha \ll 1$ gives the needle nucleation barrier and the aspect ratio

$$W = W_0(3\pi^3\alpha^3\Lambda/32\zeta)^{1/2}, \quad h/R = (3\pi\Lambda/2\alpha\zeta)^{1/2} \gg 1. \tag{10}$$

With the latter h/R, Eq. (7) becomes a transcendental equation for Λ,

$$\Lambda = \ln\sqrt{\frac{6\pi\Lambda}{\alpha\zeta}} - 1. \tag{11}$$

Equation (10) applies when $kT \ll W < W_0 - kT$ so that the nucleation barrier is significant and yet much lower than the zero-field barrier. This determines the field range

$$\tilde{E} \ll E_0 \ll \frac{W_0}{kT}\tilde{E} \equiv E_{\max}, \quad \tilde{E} \equiv \sqrt{\frac{3\pi^3\alpha^3 W_0}{32\varepsilon R_0^3}}. \tag{12}$$

For a rough guide numerical estimate, we use $\zeta \sim \alpha \sim 0.1$, which gives $h_0/\alpha R \sim 20$, $\Lambda \approx 2$, $\tilde{E} \sim 10^4$ V/cm, and $W \sim 0.3W_0$, i.e., the field-induced nucleation barrier of needle-shaped particles can be significantly lower than that of spherical particles.

Note that comparing Eqs. (5) and (10) predicts the spherical nucleation barrier to become lower than that of the needles when $E_0 \gtrsim E_{sph} \equiv \alpha^{-3/2}\tilde{E} \sim 3 \times 10^6$ V/cm. This observation reflects unequal treatment of "spheres" vs needles where the former were allowed to continuously decrease their radii with E_0, while the latter were bound from below by αR_0. It is straightforward to see that $E_0 \sim E_{sph}$ corresponds to $R \sim \alpha R_0$ for spherical particles. Assuming the same lower bound αR_0, the spherical particle nucleation barrier will exceed that of the needles under arbitrarily strong field.

Because $h/R \gg 1$, the electric field $E \sim E_0(h/R)^2$ at an embryo tip becomes strong enough to trigger secondary nucleation, quickly shunting through the rest of the amorphous structure. However, a just-formed embryo may be unstable with respect to field removal. Indeed, Eq. (8) shows that, under zero-field conditions, a long cylinder remains stable when $R > 3\pi R_0/16$. Therefore, a just-nucleated cylinder will decay unless the field is maintained long enough to grow its radius beyond $3\pi R_0/16$.

Another verifiable result of our theory is the threshold voltage switching the system within a given delay time τ.

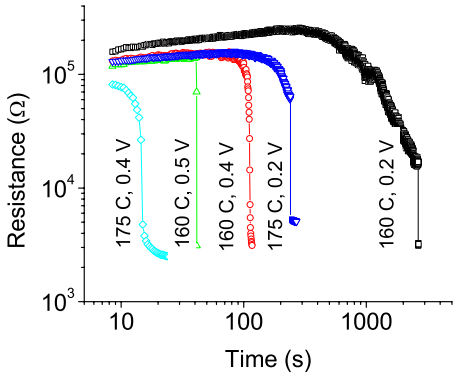

FIG. 3. (Color online) Examples of temporal variations in resistance of PCM amorphous phase under different temperatures and voltages.

Substituting ζ from Eq. (5) into Eq. (10) and using $W = kT \ln(\tau/\tau_0)$ yields the electric field, which is related to V_{th} through the amorphous layer thickness l,

$$V_{\text{th}} = \frac{V_{\max}}{\ln(\tau/\tau_0)} \quad \text{with} \quad V_{\max} = lE_{\max}. \tag{13}$$

$V_{\max}$ ($\sim$10 V for l=50 nm) corresponds to the induction time $\tau=\tau_0$. Assuming nucleation without diffusion[5,8] suggests the vibrational time $\tau_0 \sim 10^{-13}$ s, which (in combination with the experimental time $\tau \sim 100$ ns) predicts $V_{\text{th}} \sim 1.4$ V consistent with the data. This result appears quite unique as relating the observed V_{th} to the material parameters. Another characteristic voltage $\tilde{V}=\tilde{E}l \sim 0.1$ V corresponds to $W=W_0$. Below $\tilde{V}$, the nucleation switching fails, giving up to nucleation of spherical particles.

Rewriting Eq. (10) in the terms of switching delay time,

$$\tau = \tau_0 \exp\left(\frac{W_0}{kT}\frac{\tilde{V}}{V}\right) \quad \text{when} \quad V > \tilde{V}, \tag{14}$$

predicts that increasing temperature or allowing longer observation time will make switching possible under lower voltages V. Such "underthreshold" switching will be evidenced in the long lasting high resistance that eventually drops down abruptly, in the manner of standard switching. Furthermore, for low voltages $V \lesssim \tilde{V}$, our consideration predicts a qualitatively different behavior with the high-resistance state gradually decreasing due to the onset of spherical crystal nuclei forming a percolation cluster.[9]

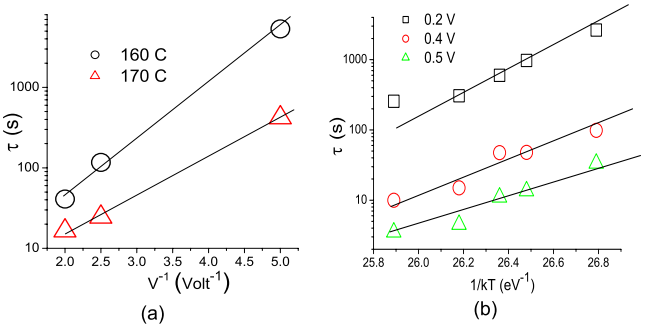

FIG. 4. (Color online) (a) Voltage dependence and (b) temperature dependence of switching delay time. Linear fits: Eq. (14).

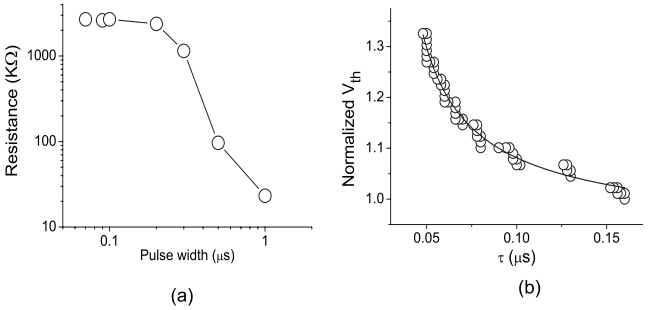

FIG. 5. (a) Stable resistance change as a function of applied voltage pulse width in the case of pulse triggered switching. The gradual decay of R corresponds to partial switching. (b) Normalized threshold voltage vs the corresponding average switching time. The curve is fit by Eq. (13).

We designed experiments continuously monitoring resistances of PCM cells put under moderate constant subthreshold voltages of 0.2, 0.4, and 0.5 V using a 4156B Semiconductor Parameter Analyzer in dc sampling mode. Measurements were done at temperatures of 160 °C, 165 °C, 167 °C, 170 °C, and 175 °C. Each condition was repeated for at least three devices and each device was tested not fewer than three times. Our PCM cells were fabricated by sputtering 100 nm GST film on top of a 80-nm-diameter contact filled with high-resistivity bottom electrode material by chemical vapor deposition. The top electrode contact was deposited on the GST layer *in situ*. Prior to the resistance measurements, all cells were reset to the high-resistance amorphous state using an HP8110A pulse/pattern generator. The amplitude of 300 ns long pulses with a trailing edge less than 4 ns was incrementally increased until the device resistance saturation.

Figure 3 shows the phenomenon of resistance abruptly dropping to crystalline state values after a certain time, which exponentially decreases with bias and temperature. (A small increase in resistances before their major drop[10] is irrelevant here.) Our thermal analysis showed that the bias-induced temperature increase was insignificant ($\lesssim$3 K) and was unable to explain the observed drop in resistances. The curves in Fig. 3 shift with bias as a whole and their represented abrupt changes in resistances look similar to the standard switching (characterized by $V_{\text{th}} \approx 1.3$ V and $\tau \gtrsim 100$ ns for our devices). These data are consistent with Eq. (14) predicting the resistance drop time exponential in temperature and voltage as verified in Fig. 4. In spite of a generally good agreement, the intersect $V^{-1}=0$ in Fig. 4(a) gives $\tau_0 \sim 1$ s, which is much higher than the assumed $\tau_0 \sim 10^{-13}$ s; a similar inconsistency of the pre-exponential obtained by extrapolating data to the region of short times is known for virtually all glasses and remains poorly understood.[11] As seen from Fig. 3, the lowest voltage (0.2 V) causes a more gradual resistance decrease resembling the behavior in devices observed under zero bias and attributed to percolation cluster of spherical nuclei.[9] We believe that the voltage 0.2 V in our experiments was close to $\tilde{V}$, consistent with its estimate above.

Also, we have verified the prediction of the short-lived low-resistive state by using voltage pulses of different widths to force the switching. As expected, a stable resistance change takes place above certain pulse width [Fig. 5(a)] showing that time under bias is not less important than the time under elevated temperature. Our observation is consistent with the fact that embryos created in strong atomic force microscope fields disappear with field removal unless their sizes exceed a certain value[12] and with the observations that turning the voltage off shortly after switching takes the system back to a resistive state.[4] Figure 5(b) shows a related experiment where shorter delay times correspond to higher V_{th} that is in agreement with Eq. (13).

In conclusion, we have developed a theory of field-induced nucleation in symmetry-breaking strong electric fields. It predicts the needle-shaped nuclei with an exponentially field-dependent nucleation rate. We have observed evidence of such a nucleation in PCM below the standard threshold voltages and over the times and temperatures significantly different from those typically reported.

Useful discussions with G. Spadini and D. Kau are greatly appreciated. We are grateful to Andrew Gordon for his invaluable help with the experimental setup. Two of us (V.G.K. and Y.A.K.) would like to acknowledge the Intel Corporation grant.

*vkarpov@physics.utoledo.edu

[1] S. Lai, Proceedings of the IEEE IEDM '03 Technical Digest (IEEE International, 2003), p. 10.1.1; G. Atwood, Science **321**, 210 (2008); A. Pirovano, A. L. Lacaita, A. Benvenuti, F. Pellizzer, and R. Bez, IEEE Trans. Electron Devices **51**, 452 (2004); A. L. Lacaita, Solid-State Electron. **50**, 24 (2006).

[2] K. Tanaka, S. Iizima, M. Sugi, and M. Kikichi, Solid State Commun. **8**, 75 (1970).

[3] S. R. Ovshinsky, Phys. Rev. Lett. **21**, 1450 (1968).

[4] D. Adler, H. Henisch, and N. Mott, Rev. Mod. Phys. **50**, 209 (1978); H. Fritzsche, in *Amorphous and Liquid Semiconductors*, edited by J. Tauc (Plenum, New York, 1974), p. 313; D. Adler, M. S. Shur, M. Silver, and S. R. Ovshinsky, J. Appl. Phys. **51**, 3289 (1980).

[5] V. G. Karpov, Y. A. Kryukov, S. D. Savransky, and I. V. Karpov, Appl. Phys. Lett. **90**, 123504 (2007); I. V. Karpov, S. D. Savransky, and V. G. Karpov, Proceedings of the 22nd IEEE Nonvolatile Semiconductor Memory Workshop, Monterey, CA, August (IEEE, Piscataway, NJ, 2007), p. 56.

[6] L. D. Landau and I. M. Lifshits, *Electrodynamics of Continuous Media* (Pergamon, New York, 1984), p. 25; V. V. Batygin and I. N. Toptygin, *Problems in Electrodynamics* (Academic, New York, 1964), p. 228.

[7] M. C. Weinberg and G. F. Nelson, J. Non-Cryst. Solids **74**, 177 (1985); C. Barrett, W. Nix, and A. Tetelman, *The Principles of Engineering Materials* (Prentice-Hall, Englewood Cliffs, NJ, 1973); X. S. Miao, L. P. Shi, H. K. Lee, J. M. Li, R. Zhao, P. K. Tan, K. G. Lim, H. X. Yang, and T. C. Chong, Jpn. J. Appl. Phys., Part 1 **45**, 3955 (2006).

[8] A. V. Kolobov, P. Fons, A. I. Frenkel, A. L. Ankudinov, J. Tominaga, and T. Uruga, Nat. Mater. **3**, 703 (2004).

[9] D.-H. Kim, F. Merget, M. Laurenzis, P. H. Bolivar, and H. Kurz, J. Appl. Phys. **97**, 083538 (2005); B. Gleixner, A. Pirovano, J. Sarkar, F. Ottogalli, E. Tortorelli, M. Tosi, and R. Bez, Proceedings of the IEEE 45th Annual International Reliability Physics Symposium, Phoenix (IEEE, Piscataway, NJ, 2007), Catalog No. 07CH37867, p. 542.

[10] I. V. Karpov, M. Mitra, D. Kau, G. Spadini, Y. A. Kryukov, and V. G. Karpov, J. Appl. Phys. **102**, 124503 (2007).

[11] L. Granasy and P. F. James, J. Non-Cryst. Solids **253**, 210 (1999); P. F. James, *ibid.* **73**, 517 (1985); V. M. Fokin, E. D. Zanotto, N. S. Yuritsyn, and J. W. P. Schmelzer, *ibid.* **352**, 2681 (2006); V. G. Karpov and D. W. Oxtoby, Phys. Rev. B **54**, 9734 (1996).

[12] T. Gotoh, K. Sugawara, and K. Tanaka, Jpn. J. Appl. Phys., Part 2 **43**, L818 (2004).